Study on Low-Thrust Stationkeeping on Geostationary Orbit

By Toshinori IKENAGA,[1)] Masayoshi UTASHIMA,[1)] Yu NAKAJIMA,[1)] Toru YAMAMOTO,[1)] Tadahiko SANO,[2)] and Noriyasu INABA[1)]

[1)]*Research and Development Directorate, JAXA, Ibaraki, Japan*
[2)]*Space Technology Directorate I, JAXA, Ibaraki, Japan*

(Received April 24th, 2017)

The primary purpose of this paper is to propose a stationkeeping method of Geostationary using low-thrust. Assuming real-time navigation is given by an on-board GPS receiver which JAXA is developing for Geostationary missions, the correction maneuver is planned through a target point method which is one of implicit guidance schemes to fly along a pre-defined nominal trajectory. Through some cases of numerical simulations in full ephemeris, the paper will reveal the feasibility of the proposed method.

Key Words: electric propulsion, geostationary orbit, target point method, stationkeeping, Next ETS

Nomenclature

$\vec{r}$	:	range vector
$\vec{v}$	:	velocity vector
F	:	thrust force
I_{sp}	:	specific impulse
t	:	time
Δt	:	time interval
J	:	cost function
$\hat{R}$	:	radial unit vector
$\hat{S}$	:	along-track unit vector
$\hat{W}$	:	cross-track unit vector
$Q(t)$	:	weighting diagonal matrix
$R(t)$	:	weighting diagonal matrix
$S(t)$	:	weighting diagonal matrix
Φ	:	state transition matrix
$\Delta\vec{V_c}(t)$	:	correction maneuver
A	:	3 x 3 submatrix
B	:	3 x 3 submatrix
C	:	3 x 3 submatrix
D	:	3 x 3 submatrix
$\vec{p}(t)$	:	position deviation
$\vec{e}(t)$	:	velocity deviation
ΔV_{plan}	:	planned delta-V
ΔV_{actual}	:	actual delta-V
A_{SAP}	:	area of solar array paddle
Cr	:	reflectivity coefficient
g	:	standard gravitational acceleration
$\vec{m_t}$	:	range deviation at epoch t

Subscripts

J2000	:	mean equator and equinox of J2000
0	:	initial epoch
c	:	correction
1	:	target epoch 1
2	:	target epoch 2
min	:	minimum
i	:	epoch *i*
T	:	transverse
thrust	:	thrusting by electric propulsion

1. Introduction

The electric propulsion system is now widely applied to many fields of space missions. One of the most important characteristics of the electric propulsion is the high specific impulse, which significantly reduces the mass of propellant consumed. The first application of an electric propulsion to a spacecraft was Zond-2/1 of the former Soviet Union in 1964, in which the on-board electric propulsion was used for the attitude control[1)]. In 1968, LES-6/1 of the United States Air Force was launched into the geostationary orbit, and the East-West stationkeeping was conducted by the on-board pulsed plasma thruster[1)]. In 2015, the ABS-3A and Eutelsat 115 West B, both of which use Boeing 702 SP bus system, were dual launched by the Space-X Falcon 9 into a super-synchronous transfer orbit whose orbital period is almost same as that of the geostationary orbit, GEO. These are the world first all-electric propulsion satellites: the on-board electric propulsion system is used for both of the transfer to, and the stationkeeping on, GEO. Japan Aerospace Exploration Agency, JAXA is also planning to develop the all-electric propulsion satellite tentatively referred as "Next Engineering Test Satellite (ETS)" to meet future needs for GEO missions[5)]. Recent progress in the all-electric satellites and GPS signal utilization on GEO has a potential to enable autonomous, precise, and efficient stationkeeping which leads to benefits on price and performance competitiveness of new-generation GEO satellites. Given such circumstances, this paper addresses on the stationkeeping method of GEO using low-thrust. Assuming the real-time navigation is given by an

on-board GPS receiver which JAXA is developing for GEO missions, the correction maneuver is planned through a target point method which is one of implicit guidance schemes to fly along a pre-defined nominal trajectory. Through some cases of numerical simulations in full dynamics, the paper will reveal the feasibility of the proposed method.

2. Dynamical Model and Coordinate System

2.1. Dynamical model

Table 1 summarizes the detail of the perturbations considered in this analysis. The orbits of the celestial bodies are determined by DE405 which is the development ephemerides released by Jet Propulsion Laboratory, JPL.

Table 1. Perturbations

Items	Description
Geo-potential	EGM96 model: 36 x 36
Air drag	not considered
SRP*	Canon ball model. Umbra/penumbra, and the variation of the Sun-Earth heliocentric distance are considered.
Third bodies	Sun, Moon, Pluto and eight planets (DE405).

* Solar Radiation Pressure

Figure 1 describes the osculating semi-major axis as a result of the orbit propagation with various perturbing forces and without active control.

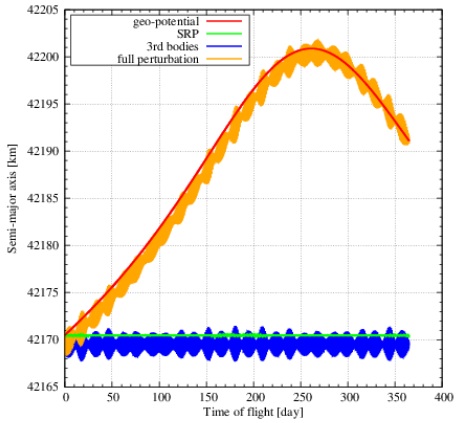

Fig. 1. Osculating semi-major axis.

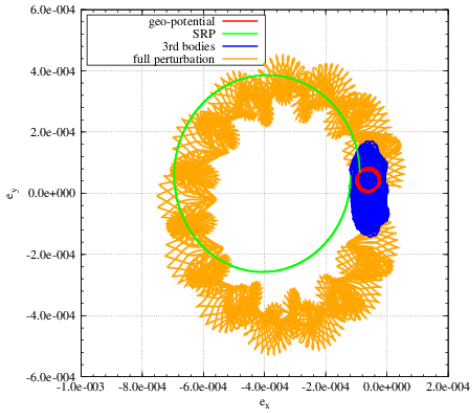

Fig. 2. Osculating eccentricity vector.

As shown Fig. 1, the semi-major axis varies by the influence of the geo-potential of Earth, which slows down the spacecraft.

Figure 2 shows the variation of the osculating eccentricity vector. As shown, the solar radiation pressure moves the eccentricity vector almost circularly.

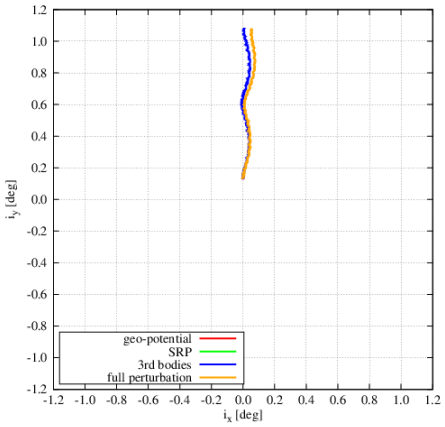

Fig. 3. Osculating inclination vector.

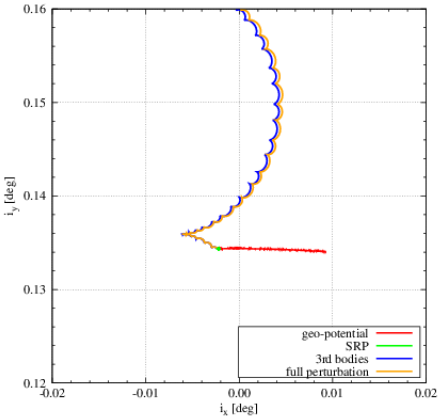

Fig. 4. Osculating inclination vector (enlarged).

Figures 3 and 4 describe the variation of the osculating inclination vector. As shown, the perturbing forces induced by the third celestial bodies changes the orbital plane of the spacecraft, which increases the inclination of the spacecraft's orbit, while the variation due to the geo-potential of the Earth or the solar radiation pressure are quite small.

2.2. Coordinate system

Two coordinate systems are used in this analysis: the mean equator and equinox of J2000 and the target point centered coordinate system "RSW" which are "radial", "along-track", and "cross-track", respectively[6]. The "RSW" coordinate system is defined as the following:

$$\hat{R} = \frac{\vec{r}_{J2000}}{\left|\vec{r}_{J2000}\right|}, \quad \hat{S} = \hat{W} \times \hat{R}, \quad \hat{W} = \frac{\vec{r}_{J2000} \times \vec{v}_{J2000}}{\vec{r}_{J2000} \times \vec{v}_{J2000}} \quad (1)$$

3. Target Point Method

The main stationkeeping algorithm is constructed based on a paper written by K. C. Howell et al. [1993][2]. This algorithm minimizes the sum of squares of correction maneuver and deviations between the nominal and estimated trajectories at the two target epochs (t_1 and t_2) in the Earth-centered mean equator and equinox of J2000. Figure 5 shows the schematic of this method. The initial state vector of the actual orbit is determined by applying the injection error at the initial epoch t_0. In this study, the same errors of GPS navigation are assumed for the injection error. Since Next-ETS is injected into the GEO by the low-thrust acceleration, it is expected that the injection errors will be order of the GPS navigation error. Note that ΔV_{actual} in Fig. 5 is the delta-V vector including the delta-V execution error in the case of chemical propulsions, however no execution error is considered here because the delta-V is finally converted to a low-thrust acceleration in this study.

At first, the state transition matrix, STM evaluated from initial epoch t_0 to certain time t ($t_0 \le t$) in the Earth-centered mean equator and equinox of J2000 is divided by four 3 x 3 submatrices as shown below in Eq. (2).

$$\Phi(t,t_0)=\begin{bmatrix} A_{tt_0} & B_{tt_0} \\ C_{tt_0} & D_{tt_0} \end{bmatrix} \tag{2}$$

The deviation between the nominal and estimated trajectories at epoch t_i ($t_0 \le t_i$) is defined as shown below in Eq. (3).

$$\vec{m}_{t_i} \cong B_{t_i t_0}\vec{e}(t_0)+B_{t_i t}\Delta\vec{V}_c(t)+A_{t_i t_0}\vec{p}(t_0) \tag{3}$$

The three vectors $p(t_0)$, $e(t_0)$, and $\Delta V_c(t)$ represent the position deviation, velocity deviation at epoch t_0, and the corrective maneuver executed at epoch t ($t_0 \le t \le t_i$), respectively. The correction maneuver, $\Delta V_c(t)$ is computed by minimizing the cost function defined by Eq. (4).

$$\begin{aligned} J\left[\vec{p}(t_0),\vec{e}(t_0),\Delta\vec{V}_c(t)\right] &= \Delta\vec{V}_c(t)^T Q(t)\Delta\vec{V}_c(t) \\ &+ \vec{m}_{t_1}{}^T R(t)\vec{m}_{t_1} + \vec{m}_{t_2}{}^T S(t)\vec{m}_{t_2} \end{aligned} \tag{4}$$

The three matrices $Q(t)$, $R(t)$, and $S(t)$ appearing in Eq. (4) are 3 x 3 weighting diagonal matrices.

The optimal corrective maneuver $\Delta V_c(t)$ at epoch t in the Earth-centered mean equator and equinox of J2000 is computed by setting the derivative of Eq. (4) by $\Delta V_c(t)$ equal to zero. The optimal corrective maneuver is expressed as shown below in Eq. (5).

$$\begin{aligned} \Delta\vec{V}_c(t) = -\Big(Q(t) &+ B_{t_1 t}{}^T R(t) B_{t_1 t} + B_{t_2 t}{}^T S(t) B_{t_2 t}\Big)^{-1} \\ &\times \Big[\Big(B_{t_1 t}{}^T R(t) B_{t_1 t_0} + B_{t_2 t}{}^T S(t) B_{t_2 t_0}\Big)\vec{e}(t_0) \\ &+ \Big(B_{t_1 t}{}^T R(t) A_{t_1 t_0} + B_{t_2 t}{}^T S(t) A_{t_2 t_0}\Big)\vec{p}(t_0)\Big] \end{aligned} \tag{5}$$

Table 2 describes the detail of the parameters defined in Target Point Method, and Figure 6 shows the flow-chart of the method. Note that the dead-band shown in Fig. 6 is defined as the relative position in RSW coordinate frame with respect to the target point.

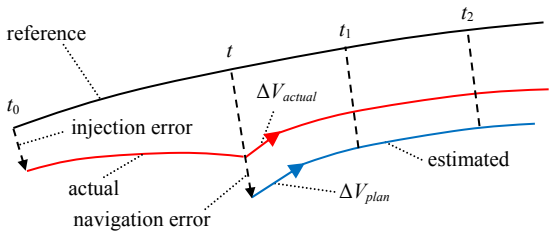

Fig. 5. Schematic of Target Point Method

Table 2. Parameters of Target Point Method

Parameter	Description
t_0	Initial epoch
t	Epoch of delta-V planning
t_1	Target epoch 1
t_2	Target epoch 2
Δt_{int1}	Time interval of delta-V planning
Δt_{int2}	Time interval to the next delta-V in case of cancellation of delta-V
Δt_1	Time interval to target epoch t_1
Δt_2	Time interval to target epoch t_2
ΔV_{min}	Minimum value of delta-V

In this paper, the on-board navigation by GPS receiver is assumed. The navigation precision assumed in this study is summarized in Table 3. In the simulation, Gaussian noises assuming the values of Table 3 are applied to produce the estimated trajectory.

Table 3. GPS navigation precision (1σ)

Items	Unit	Values
Radial position	m	15.0
Along-track position	m	2.5
Cross-track position	m	2.5
Radial velocity	m/s	0.05
Along-track velocity	m/s	0.05
Cross-track velocity	m/s	0.05

The correction maneuver for the stationkeeping is planned when the value of the position deviation from the target stationkeeping point reach 2 kilometers in each RSW coordinate axis. The location of the target point of the stationkeeping is "0.0°N and 143.0°E" and the geocentric distance is 42165.75 kilometers. The reference orbit is computed by converting the target point defined in the Earth-Centered Earth-Fixed, ECEF coordinate system to the J2000 inertial system.

Table 4 summarizes the weighting diagonal matrices for this simulation. Three different cases with different weighting matrices are simulated and compared. Note that the weighting diagonal matrices summarized in Table 4 are not optimal values.

As shown in Eq. (4), the small weight of $Q(t)$ increases the amount of the correction maneuvers, on the other hand, decreases the stationkeeping errors, and vice versa. These conflicting factors should be trade-off.

Table 4. Weighting diagonal matrices

Items		Values
Case-1	$Q(t)$	$diag(1.0\times10^{10}, 1.0\times10^{10}, 0.8\times10^{10})$
	$R(t)$	$diag(1.0, 1.0, 2.0)$
	$S(t)$	$diag(1.0, 1.0, 2.0)$
Case-2	$Q(t)$	$diag(5.0\times10^{10}, 5.0\times10^{10}, 4.0\times10^{10})$
	$R(t)$	$diag(1.0, 1.0, 2.0)$
	$S(t)$	$diag(1.0, 1.0, 2.0)$
Case-3	$Q(t)$	$diag(6.0\times10^{10}, 6.0\times10^{10}, 5.0\times10^{10})$
	$R(t)$	$diag(1.0, 1.0, 2.0)$
	$S(t)$	$diag(1.0, 1.0, 2.0)$

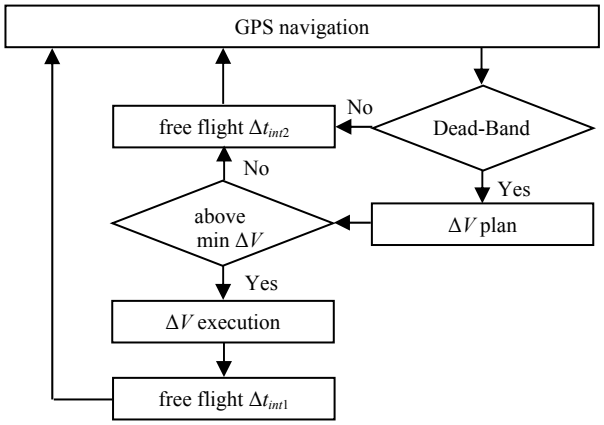

Fig. 6. Flow-Chart of Target Point Method

Once the impulsive correction maneuver is planned, the thrust duration of the electric propulsion is determined as the following:

$$t_{thrust} = \frac{\Delta V_c}{F/m} \tag{6}$$

where F is the thrust force of the electric propulsion on-board Next ETS, and m is the mass of the spacecraft at the epoch of interest. Table 5 summarizes the configuration of the spacecraft assumed in this study. A_{SAP} and m_0 appeared in Table 5 are the area of the solar array paddle exposed to the Sun direction, and the initial spacecraft's mass, respectively. Cr is the reflectivity coefficient.

Table 5. Configuration of spacecraft.

Items	Unit	Value
m_0	kg	4500.0
F	N	0.075
I_{sp}	sec	1544.0
A_{SAP}	m^2	100.0
Cr	NA	1.3

In this study, the mass of propellant consumed is computed at each integration step if the acceleration is applied.

4. Simulation

Table 6 summarizes the parameters set for the simulation. The parameters are same in all simulation cases. Note that the parameters are also not optimal values.

Table 6. Parameters set for the simulation

Parameter	Unit	Values
Δt_{int1}	day	0.15
Δt_{int2}	day	0.10
Δt_1	day	0.15
Δt_2	day	0.35
ΔV_{min}	m/s	1.0×10^{-4}

The initial epoch of the simulation is 21st/March/2024 12:00 [UTC] and the simulation duration is one-year.

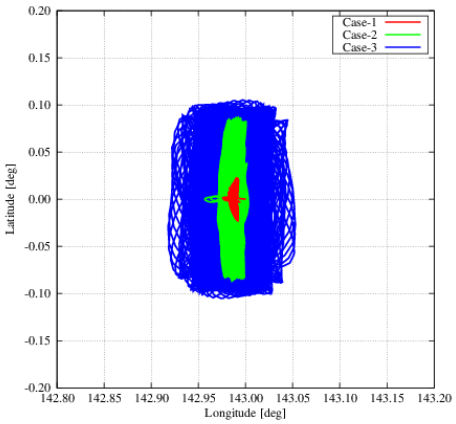

Fig. 7. Location of the spacecraft.

Figure 7 shows the location of the controlled spacecraft described in the latitude and the longitude. Figure 8 shows the orbit around the target point as viewed in RSW coordinate frame. The origin of Fig. 8 is the target point i.e., 0.0° N and 143.0° E.

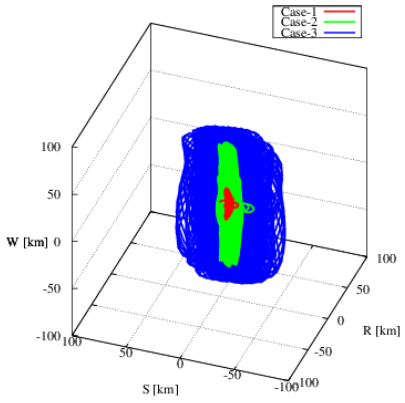

Fig. 8. Position error with respect to target point in RSW frame.

As shown in Figs. 7 and 8, the results of the simulation almost satisfy the required precision of the locations for JAXA's Next ETS i.e., ±0.1° in the latitude and the longitude.

On the other hand, Figures 9 and 10 show the time profile

of the latitude and longitude. As shown in Figs 9 and 10, the longitude of Case-3 seems to be diverging, which will not satisfy the requirement in long-term operation.

Figure 11 shows the range deviation with respect to the target point. The range deviation of Case-1 is quite small compared with the results of Case-2 and 3, which are roughly 5 to 8 times larger than that of Case-1.

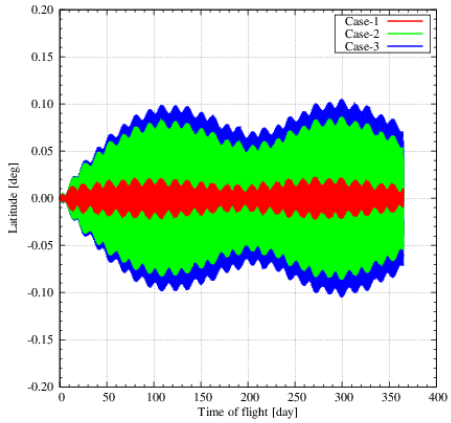

Fig. 9. Profile of Latitude.

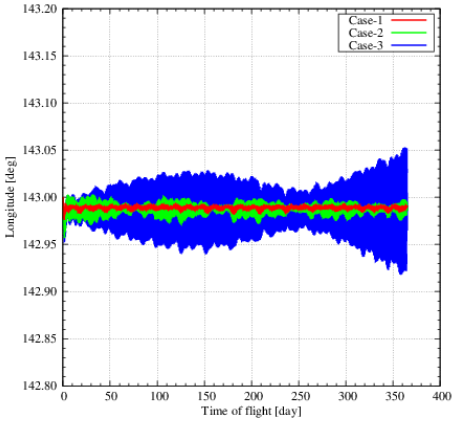

Fig. 10. Profile of Longitude.

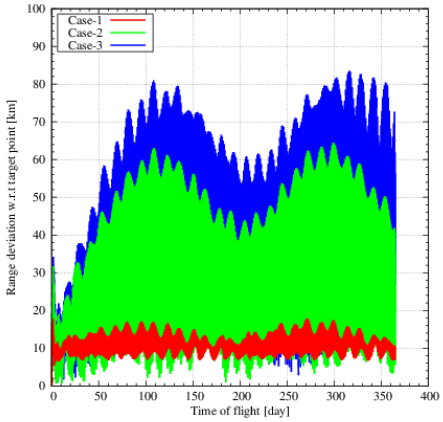

Fig. 11. Profile of Range deviation w.r.t target point.

Figure 11, 12 and 13 show the variation of the osculating semi-major axis, eccentricity and inclination vectors.

Figures 14 and 15 show the mass of propellant consumed and the thrust durations of each thrusting arc. As shown in Fig. 15, the powered flights are conducted roughly 2,000~4,000 seconds every 8,640~12,960 seconds.

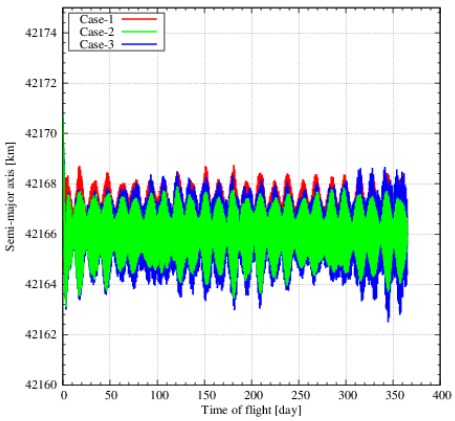

Fig. 11. Osculating semi-major axis.

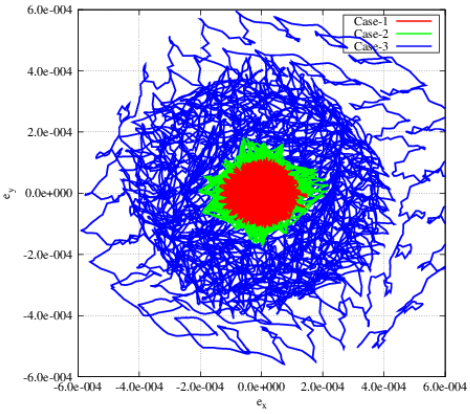

Fig. 12. Osculating eccentricity vector.

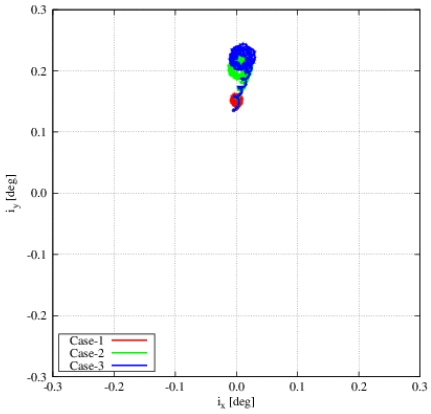

Fig. 13. Osculating inclination vector.

Table 7. Simulation results.

Items	Case-1	Case-2	Case-3
Total correction maneuvers	110.1 m/s/yr	70.5 m/s/yr	93.0 m/s/yr
Maximum longitude error	0.02°	0.04°	0.08°
Maximum latitude error	0.02°	0.04°	0.11°

Finally, Table 7 summarizes the results of the simulation. When the balance of the stationkeeping precision and cost are considered, Case-2 seems to be the best in this simulation.

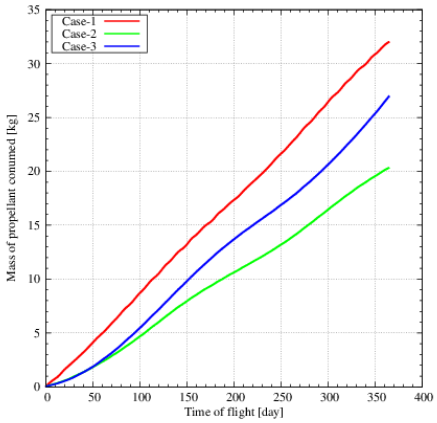

Fig. 14. Mass of propellant consumed.

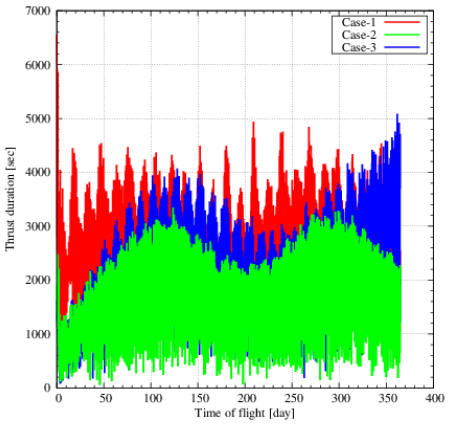

Fig. 15. Thrust duration.

5. Conclusion

This paper addresses the stationkeeping in Geostationary orbit using low-thrust continuous acceleration. The target point method developed for the halo orbit stationkeeping is employed in this study, and the simulation shows reasonable results from the perspective of the stationkeeping precision and cost. However, the simulation results show frequent orbit corrections i.e., every 2.5~3.5 hours, which may not be practical from the GPS navigation stand point. Much longer time interval between the trajectory corrections would be better. Further study is necessary to evaluate the applicability to Next ETS.

References

1) Martinez-Sanchez, M., Pollard, J. E.: *Spacecraft Electric Propulsion – An Overview*, Journal of Propulsion and Power, Vol. 14, No. 5, September-October, 1998.
2) Howell, K. C., Pernicka, H. J.: *Stationkeeping Method for Libration Point Trajectories*, Journal of Guidance, Control and Dynamics, Vol.16, No.1, January-February, 1993.
3) Kitamura, K., Suenobu, H., Yamada, K., and Shima, T.: *High-Precision Station Keeping of Geostationary Spacecraft using Analytical Mean Orbital Elements*, JSASS, Aerospace Technology, Vol. 14, pp. 113-121, 2015. (in Japanese)
4) Hirota, M.: *Long Periodic Solutions of Geostationary Orbital Plane and Eccentricity Vector by means of the General Perturbations Method*, Technical Report of National Space Development Agency of Japan, TR-16, 1983. (in Japanese)
5) Nishi, K., Nishijo, K., Ozawa, S., Sano, T., Hatooka, Y., and Fukatsu, T.: *Conceptual Design for Next Engineering Test Satellite*, 31st International Symposium on Space Technology and Science, 2017.
6) Vallado, D. A.: *Fundamentals of Astrodynamics and Applications 2nd edition*, Space Technology Library, 2004.